Environmental Earth Sciences (2024) 83:42
https://doi.org/10.1007/s12665-023-11347-7

ORIGINAL ARTICLE

Study of the spatial distribution and the temporal trend of landslide disasters that occurred in the Nepal Himalayas from 2011 to 2020

K. C. Rajan[1,2] · Keshab Sharma[3] · Bhim Kumar Dahal[1] · Milan Aryal[1] · Mandip Subedi[1]

Received: 10 June 2022 / Accepted: 29 November 2023

Abstract
Landslide disasters in Nepal are widely reported to have increased in the last decade, but there has been limited on trends in landslide occurrence in Nepal from 2011 to 2020. This study presents the spatio-temporal distribution and trends of landslide disasters in the Nepal Himalayas and identifies landslide-prone areas. Landslide disaster data was collected to assess annual variations, investigate the relation between rainfall and landslides, describe the landslide distribution pattern, conduct statistical analysis, and predict landslide causes and triggering factors. The dataset suggests that the overall trend in landslide disasters in Nepal from 2011 to 2020 is increasing, with a high level of variability in the number of landslide disasters from year to year, depending on several factors. Results show that landslide events were clustered in space and time, with 93.26% of total landslides occurring in the rainy season. The average density of landslide disasters in 2011 was 0.85 events per 1000 km^2 and increased to 3.34 in 2020. The effect of earthquake preconditioning was observed as the landslide disaster rate has been elevated since the 2015 Gorkha earthquake with systematic shifting of locations over time. Power-law relationships fit well for the cumulative frequency distribution of daily landslide disasters and the probability density of time interval between landslides. The gap between landslide events was observed as 1–170 days. Moreover, trend analysis has shown an increasing trend of landslide disasters both seasonally and annually.

Keywords Landslides · Disasters · Temporal distribution · Spatial distribution · Trend · Nepal Himalayas

Introduction

A large number of casualties, economic loss, and environmental degradation are incurred in Nepal every year. In the last decade (2011–2020), 2121 landslide disasters were reported and took the lives of 1206 people. In 2020, 493 landslide disasters claimed the lives of 303 people, 64 were missing, and 226 people were injured (Nepal DRR Portal 2020). Nepal is highly vulnerable to landslides due to its diverse geographical landscape, complex topography and geomorphology, active seismic faults, young geologic structures, and varying climatic conditions (Petley et al. 2007; Bhandary et al. 2013; Kc et al. 2021). In addition to intense rainfall during the monsoon season, urban growth, non-engineered construction in landslide-prone areas, and complex interaction of socioeconomic factors have also exacerbated terrain conditions over the last few decades, hastening the occurrence of landslides (McAdoo et al. 2018; Bhandari and Dhakal 2020; Gautam et al. 2021).

Landslide disaster casualties are often underestimated, resulting in unexpected landslide risks (Lin and Wang 2018). Observing landslides remains challenging due to their local effects and a shortage of hazard tracking networks. So, it is crucial to investigate the spatio-temporal characteristics of landslides, including their frequency, severity, and human impact (Zhang et al. 2018; Zhang and Huang 2018). Since landslides tend to reoccur in the same region (Malamud et al. 2004), investigating the spatio-temporal distributions of landslides allows identifying vulnerable locations (Dai et al. 2011; Petley 2012; Kirschbaum et al. 2015). It enhances our understanding of landslide mechanisms, landslide occurrences, and predisposing factors, which further allows us to assess and model landslide hazards, estimate denudation and

✉ Keshab Sharma
ksharma@bgcengineering.ca

1 Department of Civil Engineering, Pulchowk Campus, IoE, Tribhuvan University, Lalitpur, Nepal

2 Department of Civil Engineering, Indian Institute of Technology Kanpur, Kanpur, India

3 BGC Engineering Inc., Fredericton, NB E3C 0A9, Canada

Published online: 29 December 2023

erosion rates, develop effective geodisaster early warning systems, and provide prefeasibility data for infrastructures development (Zuo et al. 2009; Tonini and Abellan 2014; Qiu et al. 2019a, b). Existing landslides leave a lasting influence, influencing the occurrence and size of subsequent landslides, concept known as path dependency, developed by Samia et al. (2017). For instance, studies in Italy and Nepal reveal path dependency in landslides, wherein past landslide occurrences elevate the likelihood of new landslides over a 10–15 years period (Roberts et al. 2021; Samia et al. 2017; Temme et al. 2020). Thus, the study of the spatiotemporal distribution of past landslides provides a chance to determine whether areas may be prone to landslides in the future (Qui et al. 2019).

Numerous studies have examined the spatio-temporal distribution of landslides globally (Nadim et al. 2006; Petley 2012; Kirschbaum et al. 2015) and at continental scale (Sepúlveda and Petley 2015; Haque et al. 2016). Landslides were found clustered in South Asia, Southeast Asia, China, Latin America, and the Caribbean between July and September because of high rainfall. Moreover, Nepal is classified as a high-risk area on the global landslide risk chart prepared by (Nadim et al. 2006). On a national scale, Guzzetti et al. (2012), Pennington et al. (2015), Damm and Klose (2015), Pereira et al. (2016), Lin and Wang (2018) and Tonini et al. (2020) have conducted spatio-temporal studies of landslides in Italy, Britain, Germany, Portugal, China, and Italy, respectively. Although Nepal is severely affected by landslide events, few studies have been done on the distribution and trend analysis of landslides in it. Karmacharya (1989) used a spatial distribution analysis to examine the relationship between overall landslide incidents and yearly rainfall in Nepal from 1971 to 1980. The analysis showed that the landslide rate was highest in areas with higher annual rainfall. Petley et al. (2007) analyzed the landslide trend from 1978 to 2005 and concluded that the landslides effect is growing over time and is likely underrepresented as a threat in Nepal.

The conventional statistical susceptibility approaches assume that the probability of a landslide occurring remains constant over time. However, it is well-established in recent years that various factors such as climatic conditions, seismic activity, and human activities can trigger landslides. Recent studies have pointed out that climate change has caused an increase in landslide occurrences in many parts of the world (Gariano and Guzzetti 2016; Zhu et al. 2021; Jakob and Owen 2021). Burrows et al. (2023) studied the monsoon landslides in Nepal in 2015, 2017, 2018, and 2019 and identified that both spatial and temporal distribution of landslides associated with specific intense rainfall events in the region. They reported elevated number of landslides occurred in the early stage of the 2015 monsoon following the 2015 Gorkha earthquake. Jones et al. (2021) reported that the 2015 Gorkha earthquake landscape preconditioning shifted monsoon-triggered landslides in 2015 to higher slopes, reliefs, and excess topographies. The earthquake preconditioning refers to the phenomenon where landscape damage caused by earthquakes leads to a temporary increase landslide event in the region over a short period of time (Roberts et al. 2021; Jones et al. 2023). McAdoo et al. (2018) addressed relation between roads and landslides in Nepal. They reported that landslides occurred twice as frequently on terrain with poorly built roadways than terrain without roads. Similarly other extreme events such as cloud bursts and floods, have been identified as causing temporary changes in the spatial distribution of landslides (Roberts et al. 2021). Despite these observations, our understanding of how landslide spatial distributions change over time is limited due to the absence of systematic investigations.

In this regard, the study of spatial, temporal, and trend analysis of landslide occurrences using more recent data is imperative for the assessment and modelling of landslide hazards, the estimation of erosion and denudation rates, the development of efficient landslide early warning systems, land use planning and the clear understanding of historical environmental changes (Pennington et al. 2015; Damm and Klose 2015; Lin and Wang 2018; Tonini et al. 2020). Nepal still lacks a sound approach to locate areas vulnerable to landslides (Bhandary et al. 2013), a preliminary step towards landslide prevention and mitigation (Vakhshoori and Zare 2016; Pirasteh and Li 2016). This research analyses the current trend of landslide disasters between 2011 and 2020 in Nepal and their spatio-temporal distributions. A total of 2121 landslide disaster events from 2011 to 2020 were compiled to assess annual and monthly variations, distribution patterns, and spatio-temporal and trend analysis.

Study area

The high mountains in the Nepal Himalayas result from the youngest mountain-building process due to the collision of the Indian Plate and the Eurasian Plate (Dhakal 2017). Nepal has the world's highest relative relief, with a minimum elevation of 70 m and the highest 8848 m at Mount Everest's summit (Fig. 1) within 200–300 km distance from south to north. Population of the hilly and mountainous regions decreased from 49.74 to 46.36% from 2011 to 2020 (World Bank Open Data 2023). However, the urban population of Nepal increased from 17 to 21% during the same period, reflecting the ongoing urbanization trend (World Bank Open Data 2023). The country's GDP has also shown a positive trend during this period, increasing from 21.57 Billion US $ to 33.43 Billion US $. These trends demonstrate the complex relationship between population distribution, economic growth, and natural hazards in Nepal, and highlight the need for continued research

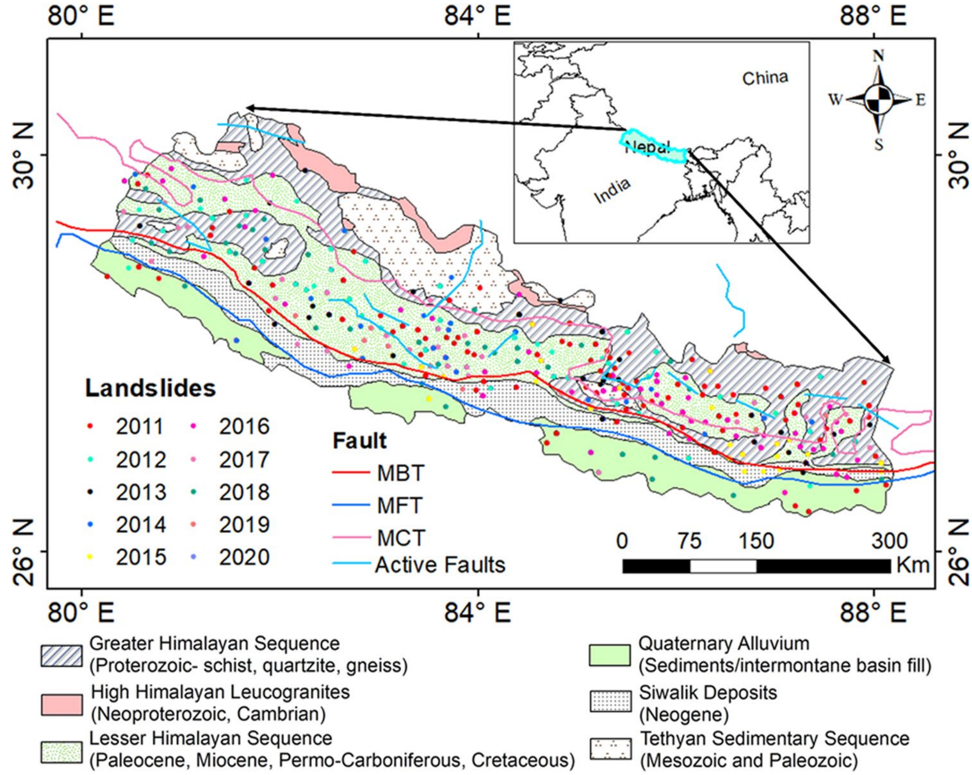

Fig. 1 Major geological zones with lithology (redrawn after Dhital (2015)) and faults in the study area

and policy efforts to manage risk and support sustainable development (World Bank Open Data 2023). With a long history of earthquakes, Nepal is one of the most seismically active places on the planet. More than 11 earthquakes greater than M_w 7.0 have been recorded since the twelfth century. More than 21,000 co-seismic landslides were observed because of the 2015 Gorkha earthquake (M_w 7.8) (Valagussa et al. 2021). Nepal is influenced by significant tectonic zones, including Tibetan-Tethys Himalaya Zone, Higher Himalaya Zone, Lesser Himalaya Zone, Sub-Himalaya (Siwalik) Zone, and Terai Zone (Dahal 2006; Sharma et al. 2018). Active tectonic faults, such as the Main Central Thrust (MCT), Main Boundary Thrust (MBT), Main Frontal Thrust (MFT), and South Tibetan Detachment System (STDS), split these tectonic zones. They are caused by the collision of the Indian and Eurasian plates (Copeland 1997); Dahal 2006). The lithology, tectonics, structures, and geological history of these tectonic zones are distinct (Pradhan et al. 2006). The Tibetan-Tethys Himalaya Zone is made up of sedimentary rock from the Cambrian to the Eocene epochs, such as shale, limestone, and sandstone. A 10 km thick sequence of severely metamorphosed coarse-grained rocks and weathered sedimentary lithologies makes up the Higher Himalaya Zone. The Lesser Himalaya contains primarily low-grade metamorphic, sedimentary, and meta-sedimentary crystalline rocks aged from the Precambrian to the Eocene (Hasegawa et al. 2009). The Sub-Himalaya Zone is composed of very thick tertiary deposits of the outer Himalayas. The deposits consist of sandstone and poorly consolidated conglomerate rock with increasing coarsening sequences.

The winter season in Nepal is primarily dry, while a significant amount of rainfall occurs in summer. The average total annual precipitation is about 1900 mm, of which 80% is concentrated during the monsoon season (i.e., May to September) (Babel et al. 2014). Temperature is highly variable across the country, depending on geography and elevation. The annual mean temperature in the country was 25.4 °C from 1973 to 2008 (Devkota 2014). The distribution of rainfall is strongly heterogeneous, both temporally and spatially. Annual rainfall ranges from < 250 to 6000 mm in the north Himalayas and central Nepal, respectively (Bhandary et al. 2013). This highly irregular rainfall trend is also a significant cause of landslide-related disasters. This region has also been hit by the cloud outburst storms in the past. Cloudburst at a time when the ground is saturated can lead to several landslides in the regions (Jones et al. 2021; Paudel and Andersen 2013).

Overall, because of rugged topography, steep relief (highly elevated mountains and deep river valleys), variable climatic conditions with high rainfall intensities, complex and young geological structures, and active tectonic processes, landslides are very common in the mountains that cover about 83% of the area of Nepal.

Material and methods

Data collection

Landslide data are the fundamental elements to analyse the spatio-temporal distribution of landslide occurrences. A dataset of landslide disasters that occurred from 2011 to 2020 (Fig. 2) was collected from Nepal Disaster Risk Reduction (DRR) catalogues. It includes the landslide disaster data as a point data set with locations reported in Ministry of Home Affairs (MoHA). The dataset contains landslide disasters that caused damage and loss of human and property occurred near human settlement areas. Thus, landslide disasters that occurred during the study period without causing any casualties or economic losses were not listed in DRR catalogues. Data (Table 1) shows the year wise number of landslide disasters, number of deaths, missing, and injured; and economic losses. Moreover, the season-wise distribution of the landslide disasters during the study period is shown in Table 2. Table 2 reveals a very strong seasonality in the occurrence of landslide disasters associated with the monsoon (a rainy season in South Asia), which in Nepal starts in summer and ends in early autumn. Since the primary focus of this research is the temporal and spatial distribution of landslide disasters, the precision with which location information was provided is adequate for this study. The standardized database was further used to derive spatial and temporal variations of landslide disasters across the country.

The rainfall data were collected from the Department of Hydrology and Meteorology (DHM). Using the annual rainfall database of 261 rain gauge stations located across the country, yearly rainfall distribution was interpolated and produced. Monthly average rainfall was derived from a dataset generated by the University of East Anglia's Climatic Research Unit (CRU) (Harris et al. 2020).

Spatial analysis

Spatial analysis was applied to deduce the spatial distribution patterns and mechanisms associated with landslides (Qiu et al. 2019a, b). Average Nearest Neighbour (ANN) and Kernel Density methods, with the help of ArcGIS, were applied to study the spatial distribution of landslide disasters across the country.

Average nearest neighbour (ANN)

The ANN algorithm determines spatial distribution (Scott and Janikas 2010) by calculating the distance between the centroids of each feature and its nearest neighbour. Then, it sums up these distances. The distribution is clustered if the average distance between two points is less than the average for a random distribution. Otherwise, the features are said to be scattered. Normal distribution probability density function was used in the analysis.

ANN is calculated by using the following relation (Eq. 1):

$$\text{ANN} = \frac{D'_O}{D'_E} \tag{1}$$

Here, D'_O denotes the average distance observed between each element and its nearest neighbour (Eq. 2):

$$D'_O = \frac{\sum_{i=1}^{n} d_i}{n} \tag{2}$$

and D'_E is the predicted mean distance between the features in a random way (Eq. 3):

$$D'_E = \frac{0.5}{\sqrt{n/A}} \tag{3}$$

where d_i is the separation from feature i to its neighbour, n is feature number, and A is the area of the smallest rectangle which encompasses all characteristics. Here, in our case, landslides are the features. The ANN z-score for the statistics is also called a global cluster indicator (Eqs. 4 and 5).

$$z = \frac{D'_O - D'_E}{\text{SE}} \tag{4}$$

where,

$$\text{SE} = \frac{0.26136}{\sqrt{n^2/A}} \tag{5}$$

If the ANN value is less than 1, the pattern shows clustering. If it exceeds 1, the trend is toward dispersion.

Kernel density

The Kernel Density method computes the density of features in their immediate vicinity (Guthrie and Evans 2004). It was used in this study to determine the magnitude of a landslide per unit area by fitting a landslide point with a smooth tapering surface using a Kernel function. The following Equation approximates the kernel density in two-dimensional space (Xie and Yan 2008; Chu et al. 2012; Cai et al. 2013; Silverman 2018) (Eq. 6):

$$\lambda(s) = \sum_{i=1}^{n} \frac{1}{\pi r^2} k\left(\frac{d_{\text{is}}}{r}\right) \tag{6}$$

where $\lambda(s)$ denotes the density of position 's'; 'n' denotes the sampling point number; 'k' represents the point 'i' weight at d_{is} distance from 's'; and finally, 'r' denotes the radius of

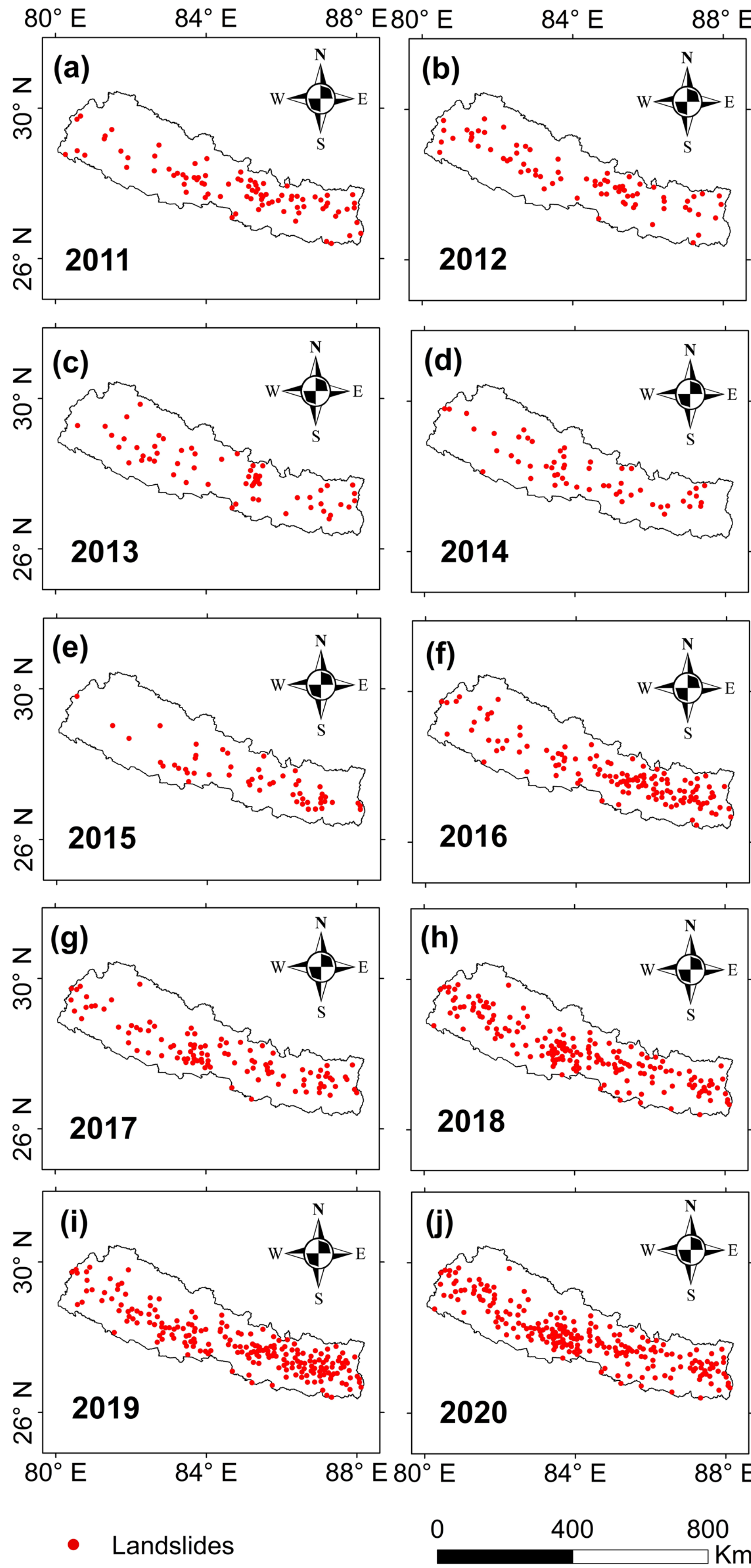

Fig. 2 Spatial distribution of landslide disasters in Nepal Himalayas, 2011–2020

Table 1 The number of landslide disasters, fatalities, and economic loss in Nepal, 2011–2020 (Nepal DRR Portal 2020)

Year	No. of landslide disasters	Deaths	Missing	Injured	Economic Loss (Million USD)
2011	126	110	24	81	0.39
2012	102	60	8	33	0.18
2013	97	87	22	57	1.44
2014	75	113	129	96	0.20
2015	62	138	13	84	0.01
2016	234	148	9	144	6.93
2017	163	70	15	56	0.53
2018	320	91	2	126	1.11
2019	449	86	11	93	3.46
2020	493	303	64	226	0.44
Total	2121	1206	297	996	14.68

Table 2 Season-wise distribution of landslide disasters in Nepal, 2011–2020

Year	Spring (Mar–May)	Summer (Jun–Aug)	Autumn (Sep–Nov)	Winter (Dec–Feb)
2011	3	105	18	0
2012	6	81	14	1
2013	3	75	17	2
2014	3	64	8	0
2015	3	54	5	0
2016	11	170	53	0
2017	13	127	19	4
2018	18	240	60	2
2019	20	343	71	15
2020	5	420	62	6
Total	85	1679	327	30

search for estimating kernel density. The kernel function used in this work was derived from the Gaussian Kernel Function (Xie and Yan 2008; Chu et al. 2012) (Eq. 7):

$$k\left(\frac{d_{is}}{r}\right) = \left\{ \begin{array}{ll} \frac{1}{\sqrt{2\pi}} \exp\left(-\frac{d_{is}^2}{2r^2}\right), & \text{if} < d_{is} \leq r \\ 0, & \text{otherwise} \end{array} \right\} \tag{7}$$

Power law relation

The total sum of frequencies greater than the daily landslide occurring at the moment can be called cumulative frequency (F_C) of daily landslides (N_L). In this scenario, the cumulative incidence can illustrate the daily occurrence of landslides over a particular amount. A power law relation (Eq. 8) was applied to estimate the cumulative landslide occurrence.

$$F_C = N_L^{\alpha} \tag{8}$$

where environment-dependent constants are denoted as C and α.

Furthermore, to assess time series, landslides occurring the same day are called single landslides. Days are used to define the time (T) between landslide occurrences. A time interval's probability density (P) denotes the relative likelihood of occurrence within specific periods. It can be used to measure and forecast the possibility of landslides (Qiu et al. 2019a, b; Qiu et al. 2020). Power law was used to represent the following relationship (Eq. 9):

$$P = DT^{\beta} \tag{9}$$

where D and β denote local conditions dependent constants.

Trend analysis

Sen's slope method

A nonparametric approach for analyzing patterns in time series suggested by (Sen 1968) is termed Sen's slope method. The formula to estimate Sen's slope is given in Eq. (10):

$$\beta = \text{Median}\left(\frac{X_j - X_i}{j - i}\right), \forall j > I \tag{10}$$

where β is the Sen's slope,X_j and X_i are the time series' elements in time j and i ($j > i$) respectively, and Median is the median feature. When the value of β exceeds 0, the time series exhibits an increasing pattern. When the value of β is less than 0, the time series shows a declining pattern.

Mann–Kendall method

The Mann–Kendall (MK) method can be defined as a nonparametric measure that does not suffer from outliers (Mann 1945; Kendall 1948). It is used for determining the importance of time series patterns (Donat et al. 2013). The formula used is shown below (Eqs. (11) and (12)):

$$S = \sum_{i=1}^{n-1} \sum_{j=i+1}^{N} \text{Sign}\left(X_j - X_i\right) \tag{11}$$

$$\text{Sign}\left(X_j - X_i\right) = \left\{ \begin{array}{c} 1(X_j - X_i) > 0 \\ 0(X_j - X_i) = 0 \\ -1\left(X_j - X_i\right) < 0 \end{array} \right\} \tag{12}$$

where 'S' is the test statistic of MK ;X_j and X_i represent the time series' 'j' and 'i' data, respectively; and the duration of the time series is 'N'.

S is raised by one if a later period's value is greater than an earlier period's value. Alternatively, S is decremented by one if the subsequent time period is less than the preceding period. Sum of these increments and decreases equals the final 'S' value (Shahid 2011). So, using Eq. (13), test statistic z is calculated to determine the existence of any statistically relevant pattern.

$$z = \begin{Bmatrix} \frac{(S-1)}{\sqrt{\frac{n(n-1)(2n+5)}{18}}} S > 0 \\ 0 S = 0 \\ \frac{(S+1)}{\sqrt{\frac{n(n-1)(2n+5)}{18}}} S < 0 \end{Bmatrix} \quad (13)$$

where z is higher than zero, the time series is ascending. If z is smaller than 0, it seems as though the time series is shrinking. Additionally, if the statistic z has an absolute value larger than 1.96, the pattern in a time series satisfies the 0.05 level of significance.

Results and discussion

Spatio-temporal distributions

The spatial distribution of landslide disasters exhibited a strong heterogeneity across the country from 2011 to 2020 (Fig. 2). The overall landslide disaster density in Nepal was 14.38 events per 1000 km^2, with an annual average of 1.44 events per 1000 km^2. It is also clear that the density of landslide disasters increased significantly from 2011 to 2020. The density of landslide disasters in 2011 was 0.85 events per 1000 km^2 and reached 3.34 events per 1000 km^2 in 2020. The data show that the density of landslide disasters is higher in the east than in the west; the density of landslide disasters decreases gradually from east to west, as shown in Fig. 2. This might be attributed to higher rainfall in the eastern part of Nepal (Kansakar et al. 2004). Figure 2f shows that, a year after the 2015 Gorkha earthquake, most landslide disasters were concentrated in the central and eastern parts of Nepal. The 2015 Gorkha earthquake and its several aftershocks caused the steep slope vulnerable to landslides, resulting in many landslides in consecutive years. The 2015 Gorkha earthquake hard hit the central and eastern parts of Nepal. The annual average landslide disaster density before and after the 2015 Gorkha earthquake was 0.42 and 1.59 events per 1000 km^2, respectively. Hundreds of earthquake-induced landslides were reported in Nepal's central and eastern parts during the 2015 Gorkha earthquake (Tiwari et al. 2017; Gautam 2017). Earthquake-induced landscape damage can lead to temporary spikes in landslide rates over annual to decadal intervals, a phenomenon known as earthquake preconditioning, first proposed by Parker et al. (2015), and developed by Marc et al. (2016). This is often a consequence of seismic damage accumulating temporarily on hillslopes, mountain ridges, and other topographic features due to the amplification of earthquake ground motion. Additionally, the locations of rainfall-triggered landslides following the 1999 Chi Chi earthquake (Lin et al. 2006), the 2005 Kashmir earthquake (Shafique 2020), the 2008 Wenchuan earthquake (Tang et al. 2016) and the 2015 Gorkha Nepal earthquake (Burrows et al. 2023; Jones et al. 2021), were observed to shift to higher slope angle, reliefs, and excess topographies. As shown in Fig. 2h–j, the largest cluster of landslide disasters in 2018, 2019 and 2020 appear to be in earthquake affected central Nepal. More detailed study is required to investigate effects earthquake preconditioning in spatio-temporal variation of the landslides disasters in Nepal.

Figure 3a shows the distributions of annual landslide disaster events and rainfall with the number of casualties from 2011 to 2020. Figure 3a shows a slow decline in landslide disasters from 2011 to 2015; however, the number of fatalities increased gently. The jump in the annual number of landslide disasters caused by the 2015 Gorkha earthquake is also seen in Fig. 3a. The higher number of landslide disasters from 2016 to 2020, compared with 2011 to 2015, was mainly associated with the 2015 Gorkha earthquake. Figure 3a showcases that the landslide hazard remains significantly higher today than on the day of the earthquake in 2015. There was no consistent relationship between the total annual landslide disasters and rainfall from 2011 to 2020. Though the annual rainfall from 2015 to 2020 was consistent, the number of landslide disasters increased since 2016.

Figure 3a shows that the annual landslide occurrence in Nepal does not solely depend on the amount of rainfall. The total landslide disaster occurrence and casualties from 2011 to 2020 showed a steady trend line. The fewest casualties occurred in 2012, when 60 people died in 102 landslide disaster events, while the most occurred in 2020 when 303 people died in 493 landslide disaster events (Table 1). Casualty numbers have been increasing over the last few years. Petley et al. (2007) also reported an increasing trend of landslides and casualties from 1978 to 2005. Some interesting patterns are evident from 2012 to 2016 and again from 2017 to 2020, when the number of landslide disasters and deaths increased continuously.

To analyse the trend of landside disasters in the last 40 years (1981–2020), an additional 30 years (1981–2010) of landslide data collected by the National Society for Earthquake Technology (NSET) from print media, reports, journals and research was combined with the study data (Fig. 3d). Two general increasing trends can be observed in the data, one from 1981 to 2002 and another from 2005 to 2020. From 1981 to 2002, landslide frequency ranges from 10 to 388 per year, with an average value of 77. From 2005 to 2020, landslide frequency significantly increased from 20

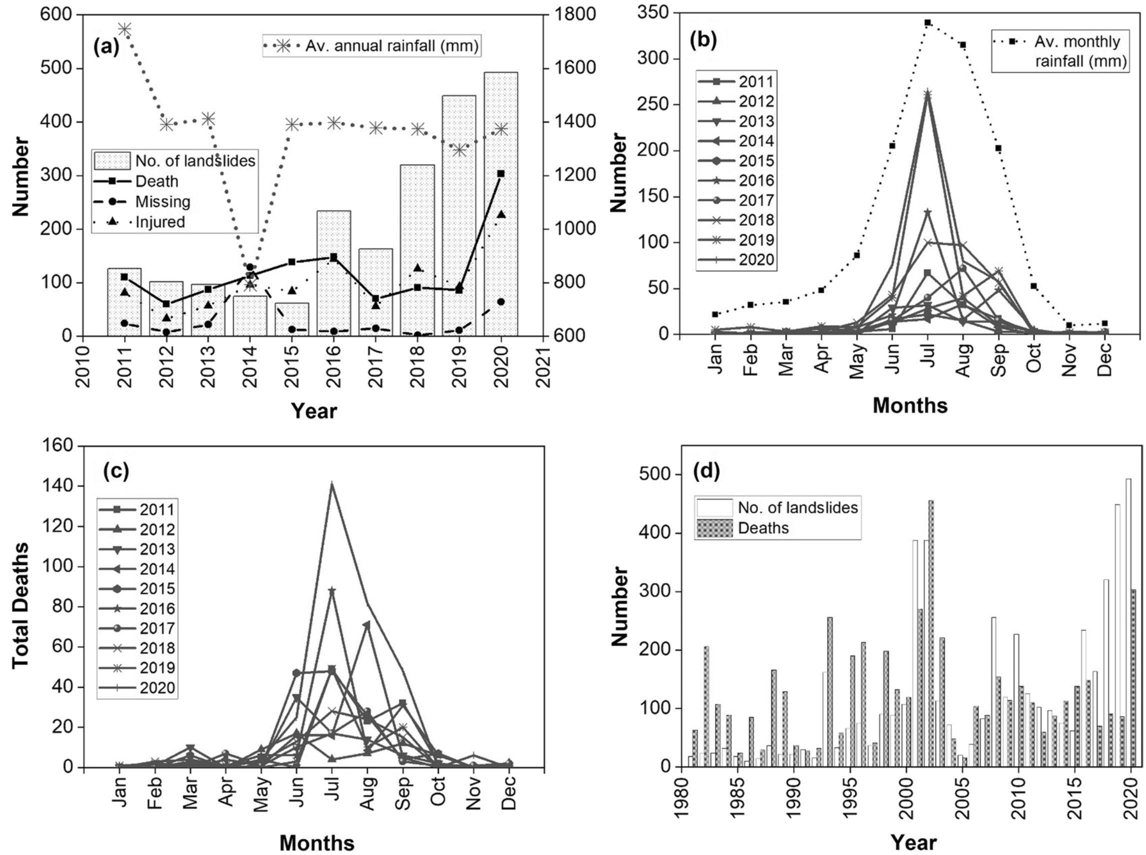

Fig. 3 Graphical representation of **a** number of landslide disaster events and deaths caused scenario for the period 1980–2020; **b** number of landslide disasters and casualties (2011–2020); **c** number of landslide disaster events (2011–2020) with average monthly rainfall (1901–2016) shown for context; and **d** month-wise total deaths caused by landslide disasters (2011–2020)

to 493 per year, with an average value of 179. The abrupt increase in landslide frequency per year after 2002 might be attributed to the human intervention in the landscape. Several studies reported that landslide frequency increased significantly due to the rapidly increased road construction and other development activities in Nepal after 2000 (Bhandary et al. 2013; Sepúlveda and Petley 2015; McAdoo et al. 2018).

The landslide disaster and rainfall monthly distributions are very consistent in terms of their peak in time, as shown in Fig. 3b. Even in Nepal, the monthly variation of landslide disasters showed that most landslides (93.26%) occurred during the rainy season, from June to September (Fig. 3b). A sharp increase in landslide occurrence was observed in July, with a slightly lower but significant number of landslides in August and September. No landslide disasters were reported from October to February, with deficient number of landslides from March to May. The monthly variation of landslide disasters and rainfall strongly indicates that rainfall is one of the triggering factors of landslides in Nepal. Dai et al. (2002) and Crosta (2004) reported that rainfall has the most significant influence on the occurrence of landslides in Nepal. Figure 3c illustrates the monthly variation of the death toll due to landslide disasters. The monthly landslide disaster events and the number of deaths follow more or less the same trend shown in Fig. 3b and c. The fatality rate was worst in July when many landslides occurred.

Figure 4a shows the fatalities due to all observed hazards versus landslide disasters during the study period. It is worth noting that landslide deaths now account for a significant portion of the total death toll. Sharp peak is seen in 2020 that align with widely reported flood and landslide events (Government of Nepal 2020). Moreover, Fig. 4b exhibits a striking resemblance to the trend variation of deaths regarding the pattern variation of economic damage due to landslide disasters. The maximum loss was observed in 2014, mainly due to the deadly Jure landslide (Ministry of Irrigation 2014). The Jure landslide buried about 1 km of Araniko Highway, a major highway leading to China, and caused the economic blockade with China.

The spatial distribution of landslide disasters on the provincial scale is shown in Fig. 5a. The list of provinces in Nepal is presented in Table 3. Koshi, Bagmati, and Gandaki Provinces were found to the landslide hotspot provinces,

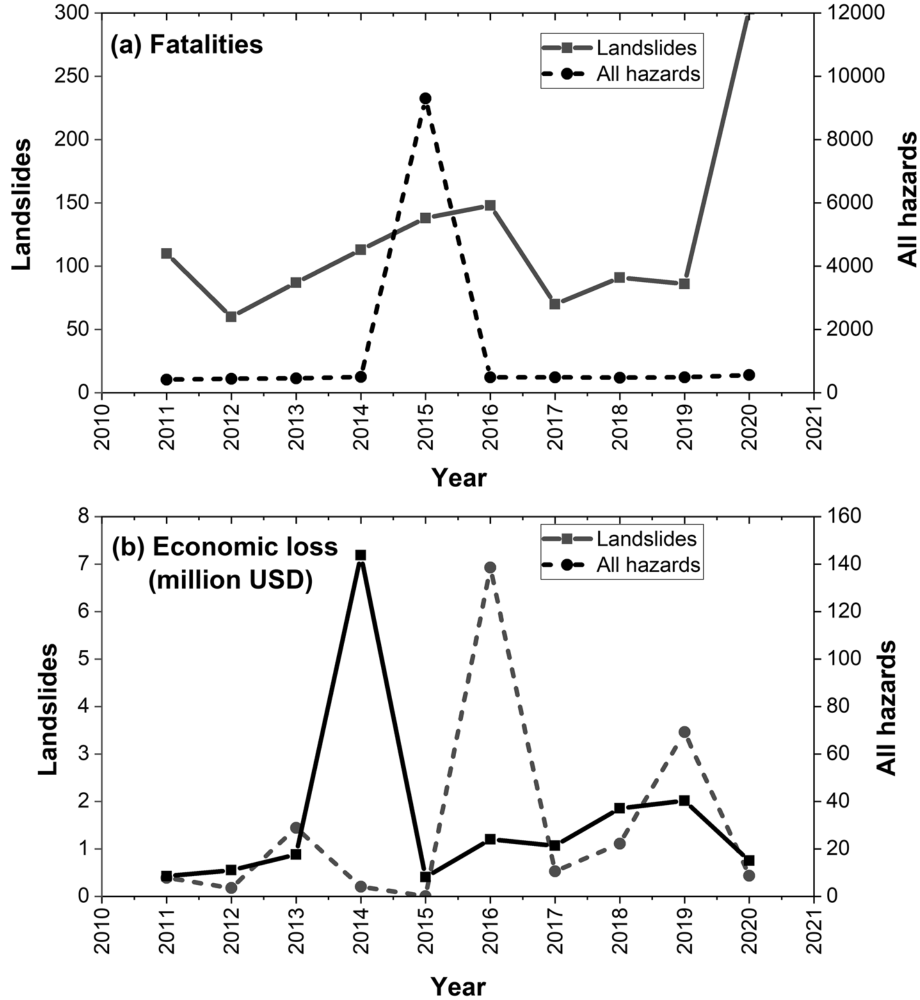

Fig. 4 **a** The number of people killed in landslide disasters and all geohazards that have been reported; **b** economic losses (in million USD) due to recorded geohazards and landslide disasters

accounting for 68.32% of landslide disasters between 2011 and 2020 (Fig. 6a), where in all cases, the percentage of landslides exceeds the percentage of land area covered. These three provinces can be properly considered as susceptible to landslide disasters. Landslide disasters occurred most in the Bagmati province, with 516 occurrences, followed by Koshi Province (488), Gandaki (445), Lumbini (240), Karnali (197), Sudurpashchim (170), and Madhesh Province (65). Based on the landforms of Nepal, there are three regions: Terai (Plains), Hilly, and Mountain. Landslide disaster distribution on these landforms is shown in Fig. 5b. Landslide disaster events were exceptionally high in the Hilly Region, especially in the central and eastern parts of the country, with 1413 events (66.62% of total landslides). The Mountain Region has 500 landslide disaster cases, followed by the Terai Region with 208 (Fig. 6b). The percentage of landslides occurred in Mountain Region (23.57%) is higher than the area of land covered by it (15%) showing higher susceptibility than two other landforms. The districts located partly within the Siwalik Hills were included in the study as landslides are known to occur there in the Terai Region. In contrast, other parts of the Terai Region, which have a slope of less than 5 degrees, are not expected to experience landslides. As shown in Fig. 6b, Terai and northwest Mountain districts have a low density of fatal landslides. This distribution seems to be dictated mainly by slope angle as well as local relief and rainfall. The Terai districts are essentially flat plains with few landslides. The distribution of landslides in the Hill and Mountain Regions is somewhat consistent with the distribution of annual rainfall, construction activities, and human settlement, which is highest in the Hill districts, especially in central and eastern Nepal.

To identify the potentially triggering factors of landslides, the relationship between the distribution of landslide disasters and influencing factors were mapped. A simplified geological map given by Carosi et al. (2013) was used for the spatial distribution study, as shown in Fig. 5c. The geological distribution of landslide disasters was mapped based on geological formation in Nepal. The map includes six geological regions: the greater Himalayan sequence, the high Himalayan leucogranites, the lesser Himalayan sequence, the Quaternary alluvium, the Siwalik deposits, and the Tethyan

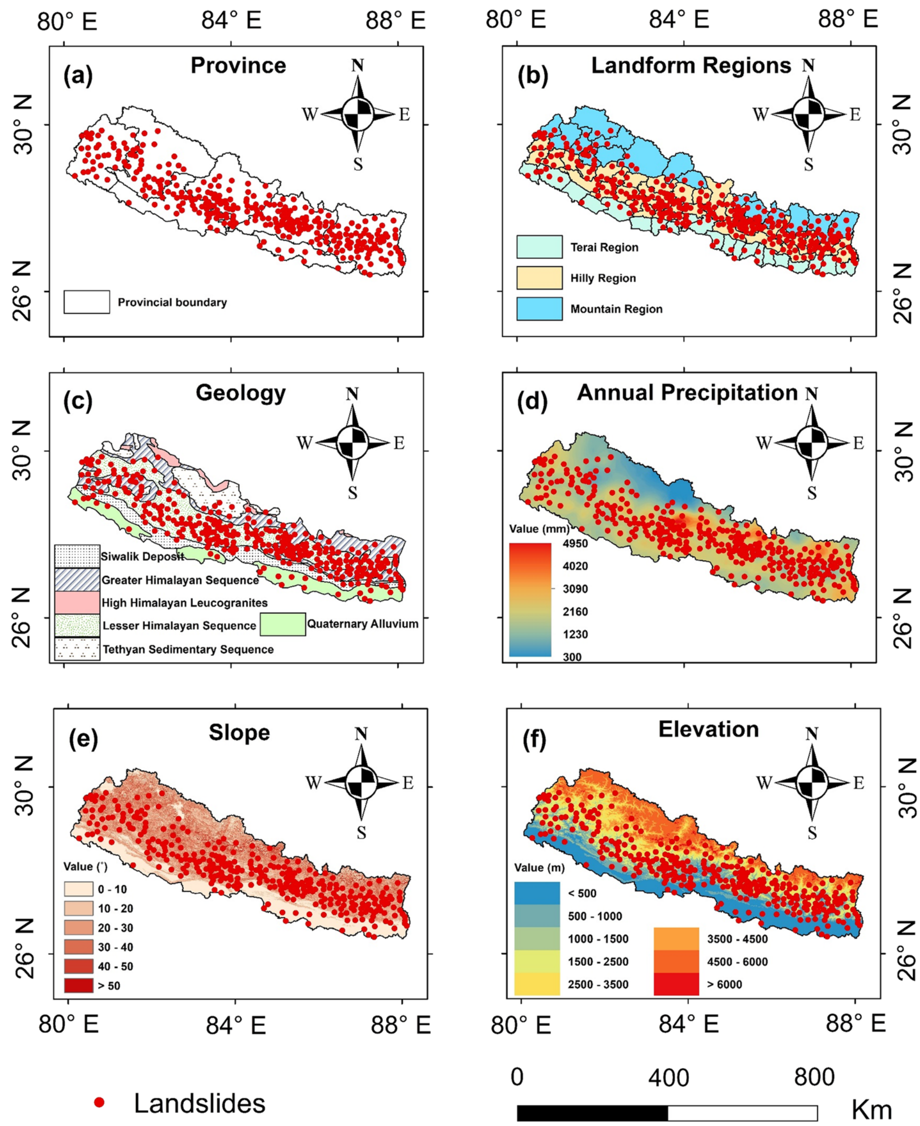

Fig. 5 Spatial distribution of landslide disasters from 2011 to 2020 presented in **a** province, **b** landform regions, **c** geological formation, **d** annual rainfall, **e** slope, and **f** elevation range scale

Table 3 The probability that an individual would be affected by landslide disasters (2011–2020)

S. No	Province	No. of Landslide disasters	Population (in thousand)	Landslide disasters per 1000 people (10^{-2})
1	Koshi	488	4534	10.76
2	Madhesh	65	5404	1.21
3	Bagmati	516	5529	9.33
4	Gandaki	445	2403	18.51
5	Lumbini	240	4499	5.33
6	Karnali	197	1570	12.54
7	Sudurpashchim	170	2552	6.66

sedimentary sequence (Fig. 5c). The Lesser Himalaya Zone has the highest number of landslide disasters (1134 events) and deaths (11), followed by the greater Himalayan sequence, the Siwalik deposits, the Tethyan sedimentary sequence, the Quaternary alluvium, and the high Himalayan leucogranites, with occurrence rates of 591, 153, 123, 109, and 11, respectively (Fig. 6c). The percentage of landslides in the Lesser Himalayan Sequence (53.47%) is significantly

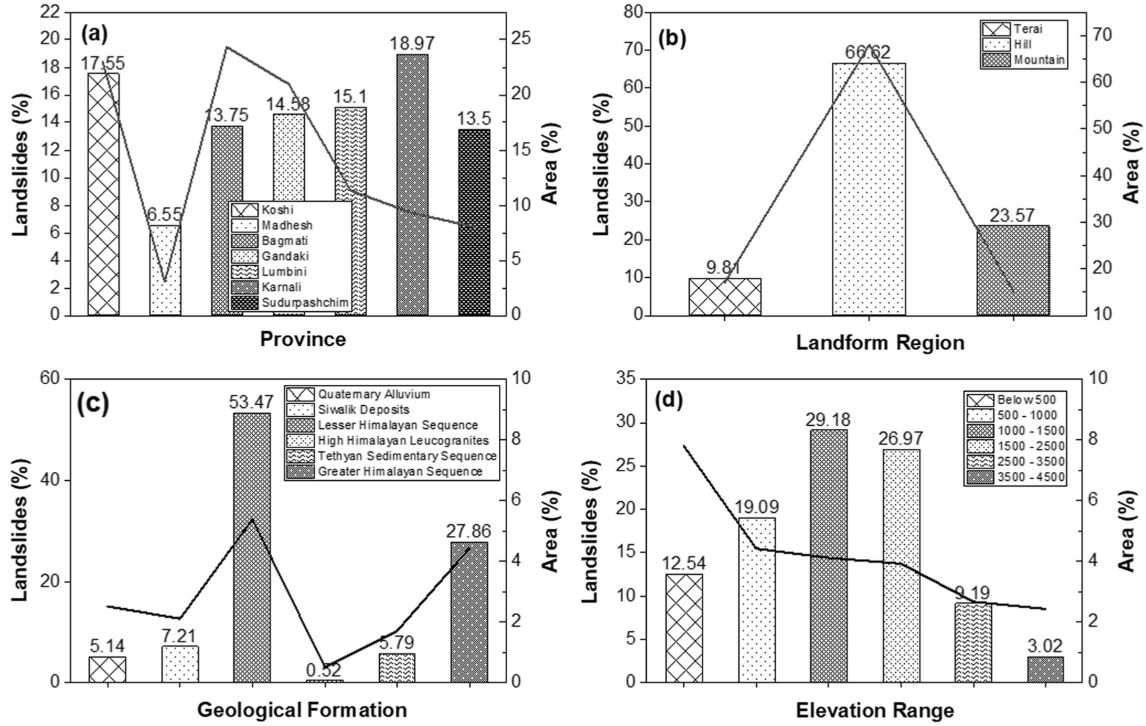

Fig. 6 Feature-wise landslide disaster distribution by **a** province, **b** landform region, **c** geological formation, and **d** elevation range

greater than the percentage of area covered by this region (32.30%). The increased susceptibility of landslides in this region can be due to the Mahabharat Range and midland area, where annual rainfall is comparatively higher, and the frequency of high-intensity rainfall is also high (Bhandary et al. 2013). Although the slopes in the midland area are gentler than in the Churia and Mahabharat Ranges, the presence of thick soil formations in slopes, weathered metasedimentary rocks, and major thrust fault systems (Hasegawa et al. 2009) makes it prone to landslides. Several studies reported that natural factors induced a few landslides, and most of them were caused by non-engineered development activities, such as road construction (Hasegawa et al. 2009; McAdoo et al. 2018). Development activities are highly concentrated in the Lesser Himalaya Zone, as this region is home to around 40% of Nepal's population (CBS 2011).

The thematic maps of slope and elevation factors were prepared using the data from digital elevation model (DEM) of resolution 30 m × 30 m provided by United State Geological Survey (USGS). Landslide disaster distribution based on rainfall intensity and slope range scale is shown in Fig. 5d and e. The landslide occurrence across the country increased significantly with the increasing slope angle. Landslide occurrence was found higher above the slope angle of 45°. However, numerous landslide disasters occurred in areas with lower slopes. This may be because anthropogenic activities mostly caused the landslides in those areas. In the Sub-Himalaya (Siwalik) Zone, more landslides was observed when the slope is greater than 15°. A rainfall intensity map was prepared using average annual rainfall data (2011–2020) from DHM. Areas with higher values of rainfall and slope angles are found to be more prone to landslide events, which is consistent with the results reported by Petley et al. (2007), Dahal et al. (2009), Dahal (2012), Timilsina et al. (2014), and Bhandari and Dhakal (2020). Similarly, on the elevation class scale, landslide distribution is high for 1000–1500 m (619 events) and 1500–2500 m (572 events) ranges (Fig. 6d), where the percentage of landslide disasters occurred is higher than the area covered by these elevation ranges. Thus, the areas in the elevation classes (1000–2500 m, as shown in Fig. 5f) with high annual rainfall were more susceptible to landslide disaster events.

Vulnerability analysis

Landslide vulnerability is a critical hazard indicator for hazard analysis and assessment since it can serve as the foundation for preventing and mitigating landslides (Corominas et al. 2014). In this case, each individual's vulnerability to landslides is considered. Additionally, a vulnerability study was conducted using the most recent demographic statistics from the 11th national census in 2011 (CBS 2011). As seen in Table 3, considering significant demographic differences between provinces, the vulnerability parameter is primarily affected by the number of landslide disasters. Bagmati, Koshi, and Gandaki provinces have been the worst affected, with many landslide disasters and comparatively high vulnerability. Lumbini also has significantly more landslide disasters, but the vulnerability is lower due to its large population. However, although having fewer landslide disasters than Lumbini, in Karnali province the vulnerability is substantial (12.54×10^{-2}) due to its tiny population (the lowest of Nepal's provinces). Among all provinces, the landslide occurrences and vulnerability value are minimal in Madhesh province.

Spatial analysis

Average nearest neighbour (ANN)

Figure 7 depicts the significant degree to which the geographical distribution pattern of landslides is reliant on distinct z-scores. In general, z-scores with smaller values suggest a more concentrated spatial distribution of landslides, while z-scores of larger values show a more distributed spatial distribution. The p-value estimates the region under the curve for a defined distribution, according to limitations imposed by the test statistic. The findings indicated that the ANN ratio is 0.046, less than one, from 2011 to 2020. This result showed that the research area's landslide points are clustered.

Additionally, the *z*-score is − 84.021, which is smaller than the value of − 2.58. At the 0.01 significance mark, this finding showed that landslide disasters considered in this study were clustered spatially. Similarly, the ANN and z-score for all years are calculated, and observed landslide disasters are grouped around a 0.01 level of significance (Table 4). Guthrie and Evans (2004) and Qiu et al. (2019a, b) have similar results of landslide-clustering phenomena using nearest neighbour analysis.

Kernel density

Landslide intensity, or spatial density, refers to the number of landslides in a given area. Using kernel density estimation, we developed a map of landslide intensity based on Eqs. (7) and (8) (Fig. 8). The findings indicated that landslide disaster distribution was highly clustered and heterogeneous.

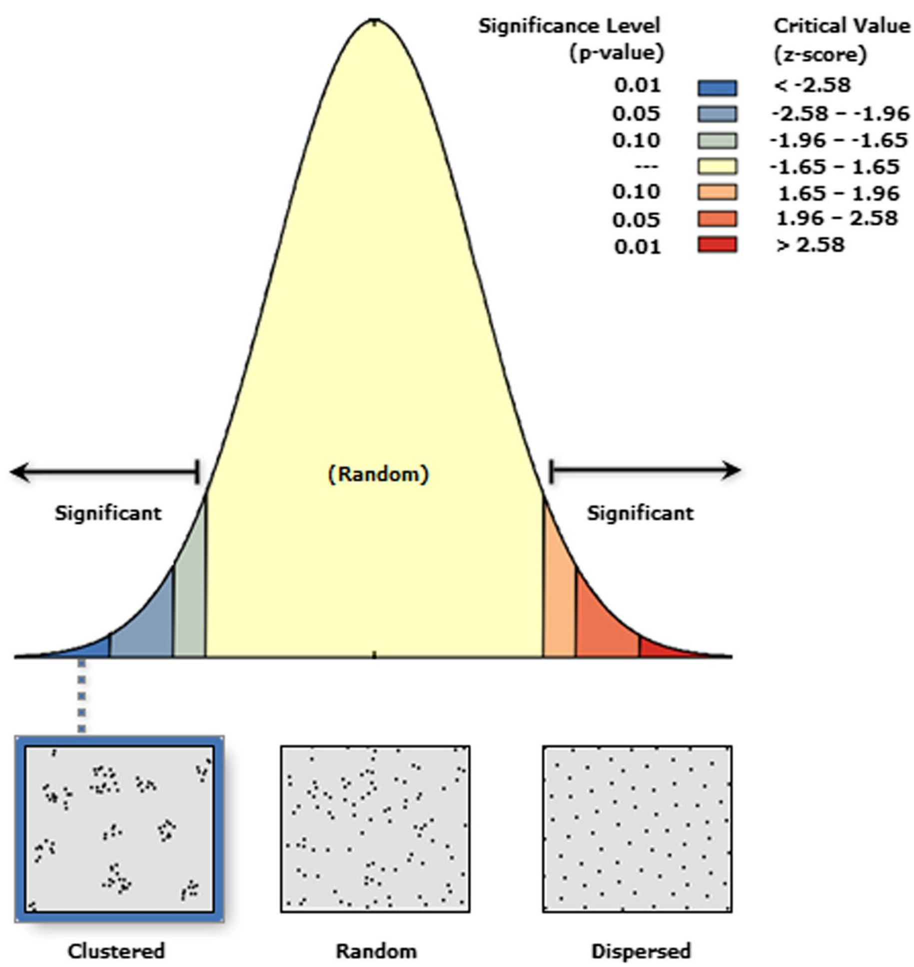

Fig. 7 Spatial patterns of landslide disasters in Nepal (2011–2020)

Table 4 Summary of average nearest neighbour (ANN) analysis for landslide disasters (2011–2020)

S. No.	Year	ANN ratio	*z*-score
1	2011	0.437	− 12.081
2	2012	0.578	− 8.156
3	2013	0.502	− 9.382
4	2014	0.545	− 7.532
5	2015	0.673	− 4.932
6	2016	0.436	− 16.493
7	2017	0.559	− 10.761
8	2018	0.445	− 19.009
9	2019	0.363	− 25.831
10	2020	0.351	− 27.559
11	2011–2020	0.046	− 84.021

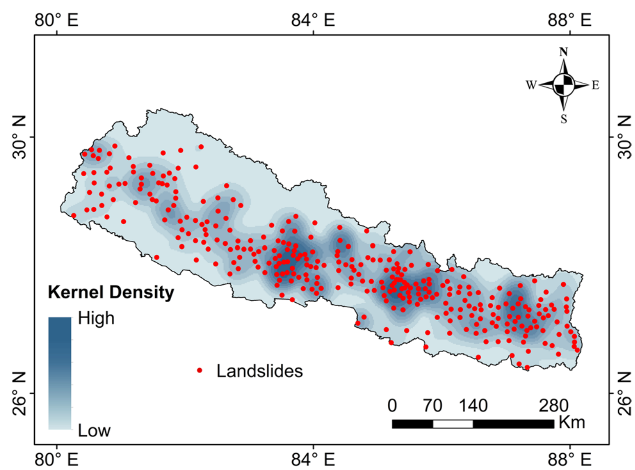

Fig. 8 Mapping of landslide intensity using kernel density analysis (2011–2020)

Results from kernel density analysis are in accordance with the earlier findings on ANN. Numerous landslide disasters occurred in evident concentrated areas. On the other hand, there were a few landslide disasters in places that were not prone to landslides. Most of these happened in the central-east portion, with just a handful occurring in the northwest portion. Landslide occurrences declined steadily from the country's central-east and northwest regions.

Power-law relation

Landslides registered in a single day (N_L) acted as a proxy for the number of landslides over time. Between 2011 and 2020, Nepal experienced 758 days with an average of $1 \leq N_L \leq 47$ landslide disasters per day. Numerous days in this time series contain 0 values, indicating no landslides. Single landslide-occurring days made up about 52.63% of all landslide event days. We plotted the cumulative frequency distribution of regular landslides on log–log axes. As shown in Fig. 9a, the cumulative distribution shrank dramatically as the number of landslide disasters every day. The cumulative frequency distribution of regular landslides in Nepal is best represented by the following inverse power law function, as seen in Eq. (14).

$$F_C = 95.49\,N_L^{-1.81}\left(R^2 = 0.974\right) \tag{14}$$

Rossi et al. (2010) and Qiu et al. (2019a, b) also demonstrate that the cumulative frequency of landslides each day is distributed as a power-law with some negative scaling component. Moreover, landslide recurrence can be determined using time interval regression (Qiu et al. 2019a, b). As a result, we examined the time intervals

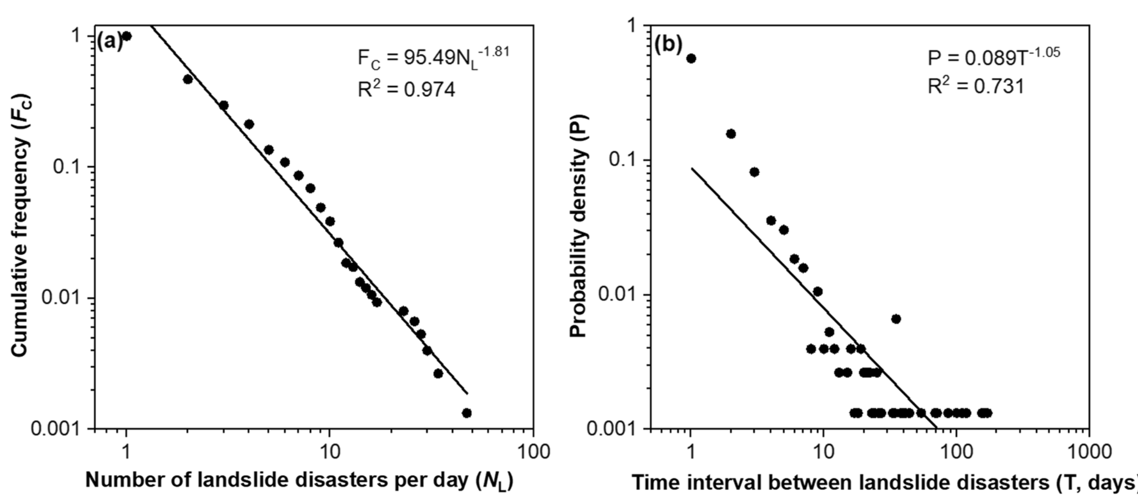

Fig. 9 Power law relationship between **a** F_C and N_L **b** P and T

between landslide disaster occurrences. The time interval between landslide disaster events was between 1 and 170 days. This result showed that the landslide disasters occurred regularly in the sample area, with an average of approximately 5 days between occurrences. A one-day time interval accounted for 57.19% of all periods between landslide disasters. This suggests that the frequency and non-random distribution of landslide occurrences occurred throughout time. The results (Fig. 9b) showed a strong power-law relation of the probability density (P) with the time differences between landslide disasters (T), as shown in Eq. (15):

$$P = 0.089\,T^{-1.05}\left(R^2 = 0.731\right) \tag{15}$$

Many researchers (like Guzzetti et al. (2005), Blender et al. (2008), and Witt et al. (2010)) have presented that the probability distribution of time differences series follows Poisson, binomial, Weibull, and exponential distributions. However, the time series distribution of this study area resembled a power-law function, as coherent with the findings by (Qiu et al. 2019a, b) proposed for the Qinba Mountains in China.

Trend analysis

Sen's slope method

For the current study, trend analysis of landslides in Nepal was done for ten years of time series data (2011–2020) on a seasonal and annual basis. It is evident from Fig. 10 that the maximum landslide events occurred in summer. It has also been observed that landslides during winter were lower than in all other seasons. Values of β for spring, summer, autumn, and winter were obtained as 2, 35, 6, and 0.5, respectively, revealing a positive (increasing) trend. The top increasing trend has been shown in summer season data, whereas the minimum was found in winter. The annual trend analysis of landslides is shown in Fig. 11. It has also shown an increasing trend of landslide occurrence with increasing time, as consistent with reporting by (Petley et al. 2007).

Mann–Kendall method

When MK-test findings in Table 5 are analyzed, it is clear that all seasonal and annual trends exhibit an increasing pattern, with a z-value greater than 0. Additionally, the autumn

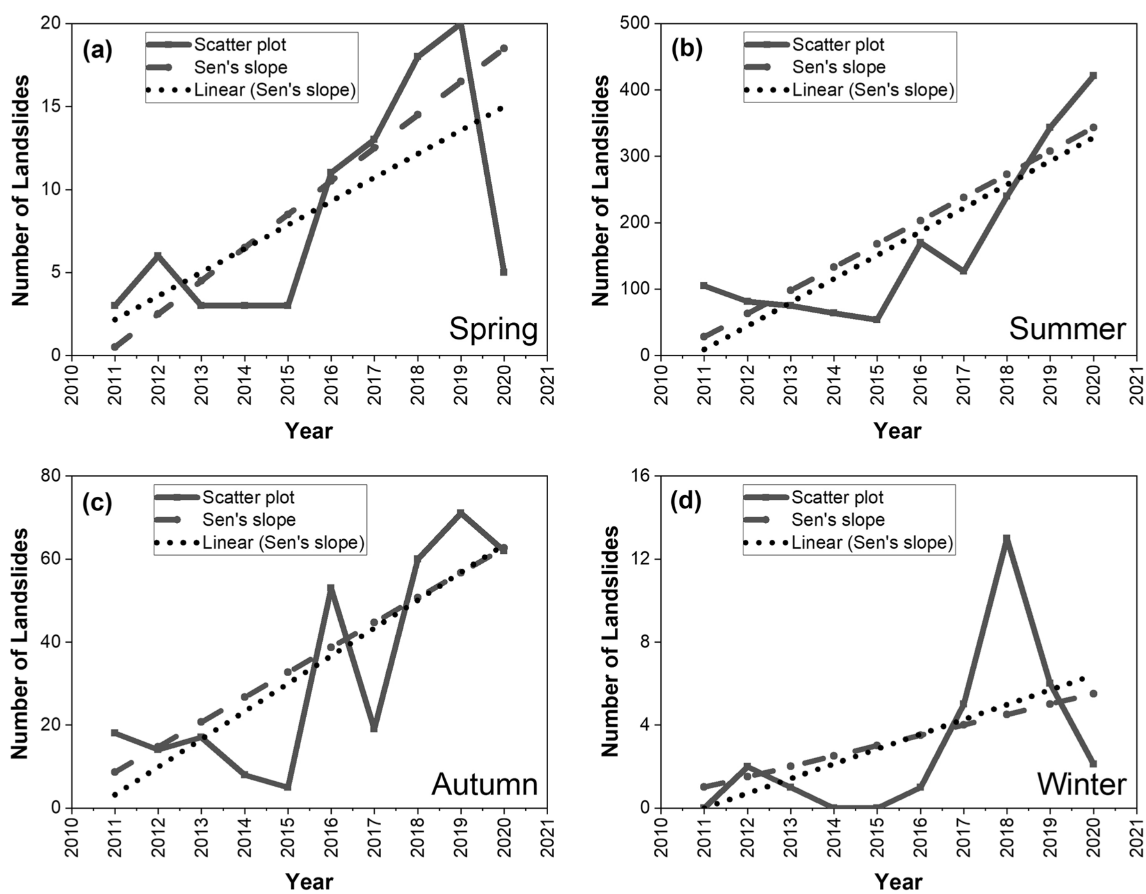

Fig. 10 Seasonal landslides trend analysis (2011–2020) **a** spring, **b** summer, **c** autumn, and **d** winter

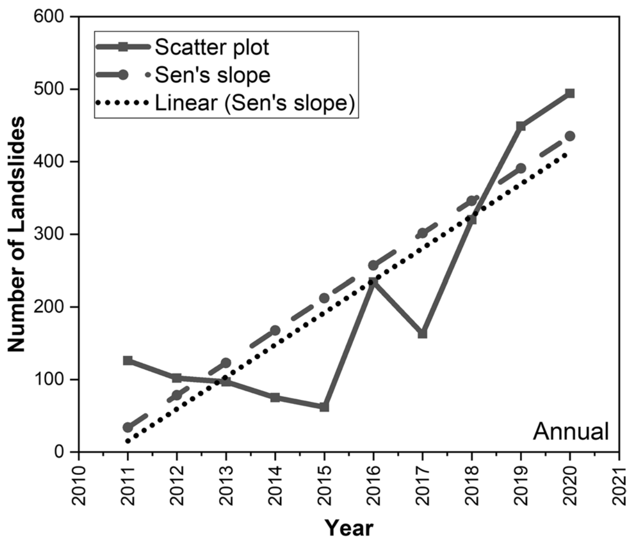

Fig. 11 Annual trend analysis of landslides (2011–2020)

season has a z-value marginally more than 1.96, i.e., the pattern in the time series is significant at the 0.05 mark. Thus, this finding agrees with the results from Sen's slope analysis. It is interesting to note that, with a strong coherence to the findings of this study, Petley et al. (2007) and Froude and Petley (2018) speculate that an increase in monsoon rains over central Nepal may at least be partially responsible for an overall increase in landslides in the country.

Conclusions

The study of spatio-temporal distributions of landslides disaster is becoming instrumental for understanding landslide hazards and risk, land use planning and sustainable development activities. The spatio-temporal distribution and trend in landslide disaster occurrence from 2011 to 2020 were analyzed for Nepal. The major conclusions drawn are as follows:

- Nepal is experiencing an increase in landslide disasters. Landslide density was 0.85 events/1000 km^2 in 2011 and reached 3.34 events/1000 km^2 in 2020, with an average increasing rate of 0.25 events/1000 km^2/year.
- The spatial variation of landslide disasters varies greatly between provinces and geological areas. The probability of each person suffering landslide disasters is highest in Gandaki province, followed by Karnali and Koshi Province, and minimum in Madhesh Province. The Lesser Himalaya Zone was highly vulnerable to landslide disasters due to its geographical formations, steep slopes, rainfall intensity, and non-engineered development activities.
- Rainfall mainly controls the monthly distribution of landslide disasters. A strong correlation between landslide occurrence and the monsoon (rain season) has been observed. The results showed that about 93.26% of landslide disasters (1978 events) occurred during the monsoon in Nepal.
- After 2015, there is a dramatic increase in landslide disasters, attributed to the M_w 7.8 Gorkha earthquake in Nepal. Landslide disaster rates remain elevated in several provinces several years after the earthquake. The earthquake mainly triggered landslides in the central east areas. Landslide disasters in the 14 worst-affected districts remains significantly higher than on the day of the earthquake in 2015.
- Our analysis illustrates that the nature of landslide disasters has significantly changed since the 2015 Gorkha earthquake. The sequential mapping demonstrates that the location of landslide activity has shifted systematically over time to the earthquake devasted areas. More details analysis is required to investigate the effect of earthquake preconditional on spatio-temporal variation of landslides disaster.
- During the study period, Nepal experienced 758 days with an average of $1 \leq N_L \leq 47$ landslide disasters per day, with a single landslide event accounting for 52.63% of all days of landslide events.
- In the context of Nepal, the data indicates that the probability density (P) exhibits a significant power-law relationship with the time interval between landslide disaster occurrences (T), which can be used to measure and forecast the possibility of landslide disasters.
- Trend analysis has revealed the positive (increasing) trend of landslide occurrence. With maximum positive Sen's slope value, the summer season shows the maximum number of landslide events and a maximum increasing trend.

Table 5 Seasonal trend analysis results for Mann–Kendall test

S. N	Mann–Kendall test parameters	Spring	Summer	Autumn	Winter	Annual
1	Mk test statistics (s)	9	14	23	20	10
2	Var (s)	91	92	125	119.33	92
3	z	0.84	1.36	1.97	1.74	0.94
4	Trend at 0.05 significant level	No	No	Positive	No	No

With increasing development activities and climate change effects in Nepal, landslide disasters continue to increase and affect people's lives and property. Therefore, the Nepal government should formulate the required policies and take immediate actions to reduce the landslide disasters in Nepal. Statistical study like this is helpful for policymakers, planners, and engineers engaged in landslide disaster management in Nepal.

Author contributions Conceptualization, RK, BKD and KS; methodology, RK, MA, MS and BKD; software, RK and MA.; validation, RK, BKD, MS and KS; formal analysis, RK and MA; investigation, RK; data curation, RK and MA; writing—original draft preparation, RK; writing—review and editing, BKD, MS and KS; supervision, BKD, MS and KS. The published version of the work has been reviewed and approved by all authors.

Funding The authors declare that no funds, grants, or other support were received during the preparation of this manuscript.

Data availability Data may be available on demand.

Declarations

Conflict of interest The authors declare that they have no known competing financial interests or personal relationships that could have appeared to influence the work reported in this paper.

References

Babel MS, Bhusal SP, Wahid SM, Agarwal A (2014) Climate change and water resources in the Bagmati River Basin Nepal. Theoret Appl Climatol 115(3–4):639–654. https://doi.org/10.1007/S00704-013-0910-4/TABLES/9

Bhandari BP, Dhakal S (2020) Spatio-temporal dynamics of landslides in the sedimentary terrain: a case of Siwalik zone of Babai watershed Nepal. SN Appl Sci 2(5):1–17. https://doi.org/10.1007/s42452-020-2628-0

Bhandary NP, Yatabe R, Dahal RK, Hasegawa S, Inagaki H (2013) Areal distribution of large-scale landslides along highway corridors in central Nepal. Georisk 7(1):1–20. https://doi.org/10.1080/17499518.2012.743377

Blender R, Fraedrich K, Sienz F (2008) Extreme event return times in long-term memory processes near 1/*f*. Nonlinear Process Geophys 15(4):557–565. https://doi.org/10.5194/NPG-15-557-2008

Burrows K, Marc O, Andermann C (2023) Retrieval of monsoon landslide timings with Sentinel-1 reveals the effects of earthquakes and extreme rainfall. Geophys Res Lett 50(16):e2023GL104720. https://doi.org/10.1029/2023GL104720

Cai X, Wu Z, Cheng J (2013) Using kernel density estimation to assess the spatial pattern of road density and its impact on landscape fragmentation. Int J Geogr Inf Sci 27(2):222–230. https://doi.org/10.1080/13658816.2012.663918

Carosi R, Montomoli C, Iaccarino S, Visonà D (2013) Tectono-metamorphic discontinuities in the Greater Himalayan Sequence and their role in the exhumation of crystalline units. Springer, p 6564

Chu HJ, Liau CJ, Lin CH, Su BS (2012) Integration of fuzzy cluster analysis and kernel density estimation for tracking typhoon trajectories in the Taiwan region. Expert Syst Appl 39(10):9451–9457. https://doi.org/10.1016/j.eswa.2012.02.114

Copeland P (1997) The when and where of the growth of the Himalaya and the Tibetan Plateau. Tectonic uplift and climate change. Springer, pp 19–40

Corominas J, van Westen C, Frattini P, Cascini L, Malet JP, Fotopoulou S, Catani F, Van Den Eeckhaut M, Mavrouli O, Agliardi F, Pitilakis K, Winter MG, Pastor M, Ferlisi S, Tofani V, Hervás J, Smith JT (2014) Recommendations for the quantitative analysis of landslide risk. Bull Eng Geol Environ 73(2):209–263. https://doi.org/10.1007/s10064-013-0538-8

Crosta GB (2004) Introduction to the special issue on rainfall-triggered landslides and debris flows. Eng Geol 73(3–4):191–192. https://doi.org/10.1016/J.ENGGEO.2004.01.004

Dahal RK (2012) Rainfall-induced Landslides in Nepal. Int J Eros Control Eng 5(1):1–8. https://doi.org/10.13101/ijece.5.1

Dahal RK, Hasegawa S, Yamanaka M, Dhakal S, Bhandary NP, Yatabe R (2009) Comparative analysis of contributing parameters for rainfall-triggered landslides in the Lesser Himalaya of Nepal. Environ Geol 58(3):567–586. https://doi.org/10.1007/s00254-008-1531-6

Dai FC, Lee CF, Ngai YY (2002) Landslide risk assessment and management: an overview. Eng Geol 64(1):65–87. https://doi.org/10.1016/S0013-7952(01)00093-X

Dai FC, Xu C, Yao X, Xu L, Tu XB, Gong QM (2011) Spatial distribution of landslides triggered by the 2008 Ms 8.0 Wenchuan earthquake China. J Asian Earth Sci 40(4):883–895. https://doi.org/10.1016/j.jseaes.2010.04.010

Damm B, Klose M (2015) The landslide database for Germany: closing the gap at national level. Geomorphology 249:82–93. https://doi.org/10.1016/j.geomorph.2015.03.021

Devkota RP (2014) Climate change: trends and people's perception in Nepal. J Environ Prot 5(4):255–265. https://doi.org/10.4236/JEP.2014.54029

Dhakal S (2017) Geological divisions and associated hazards in Nepal. Contemporary Environmental Issues and Methods in Nepal, pp 100–109

Dhital M (2015) Geology of the Nepal Himalaya: regional perspective of the classic collided orogen. Geol Nepal Himal. https://doi.org/10.1007/978-3-319-02496-7

Donat MG, Alexander LV, Yang H, Durre I, Vose R, Caesar J (2013) Global land-based datasets for monitoring climatic extremes. Bull Am Meteorol Soc 94(7):997–1006. https://doi.org/10.1175/BAMS-D-12-00109.1

Froude MJ, Petley DN (2018) Global fatal landslide occurrence from 2004 to 2016. Nat Hazard 18(8):2161–2181. https://doi.org/10.5194/NHESS-18-2161-2018

Gariano SL, Guzzetti F (2016) Landslides in a changing climate. Earth Sci Rev 162:227–252. https://doi.org/10.1016/J.EARSCIREV.2016.08.011

Gautam D (2017) Unearthed lessons of 25 April 2015 Gorkha earthquake (MW 7.8): geotechnical earthquake engineering perspectives. Geomat Natl Hazards Risk 8(2):1358–1382. https://doi.org/10.1080/19475705.2017.1337653

Gautam P, Kubota T, Sapkota LM, Shinohara Y (2021) Landslide susceptibility mapping with GIS in high mountain area of Nepal: a comparison of four methods. Environ Earth Sci 80(9):359. https://doi.org/10.1007/s12665-021-09650-2

Government of Nepal (2020) Nepal: floods and landslides. https://Reliefweb.Int/Disaster/Fl-2020-000165-Npl

Guthrie RH, Evans SG (2004) Magnitude and frequency of landslides triggered by a storm event, Loughborough Inlet, British Columbia. Natl Hazards Earth Syst Sci 4(3):475–483. https://doi.org/10.5194/nhess-4-475-2004

Guzzetti F, Reichenbach P, Cardinali M, Galli M, Ardizzone F (2005) Probabilistic landslide hazard assessment at the basin scale. Geomorphology 72(1–4):272–299. https://doi.org/10.1016/J.GEOMORPH.2005.06.002

Guzzetti F, Mondini AC, Cardinali M, Fiorucci F, Santangelo M, Chang KT (2012) Landslide inventory maps: new tools for an old problem. Earth-Sci Rev 112(1–2):42–66. https://doi.org/10.1016/j.earscirev.2012.02.001

Haque U, Blum P, da Silva PF, Andersen P, Pilz J, Chalov SR, Malet JP, Auflič MJ, Andres N, Poyiadji E, Lamas PC, Zhang W, Peshevski I, Pétursson HG, Kurt T, Dobrev N, García-Davalillo JC, Halkia M, Ferri S, Keellings D (2016) Fatal landslides in Europe. Landslides 13(6):1545–1554. https://doi.org/10.1007/s10346-016-0689-3

Harris I, Osborn TJ, Jones P, Lister D (2020) Version 4 of the CRU TS monthly high-resolution gridded multivariate climate dataset. Sci Data 7(1):109. https://doi.org/10.1038/s41597-020-0453-3

Hasegawa S, Dahal RK, Yamanaka M, Bhandary NP, Yatabe R, Inagaki H (2009) Causes of large-scale landslides in the Lesser Himalaya of central Nepal. Environ Geol 57(6):1423–1434. https://doi.org/10.1007/s00254-008-1420-z

Jakob M, Owen T (2021) Projected effects of climate change on shallow landslides, North Shore Mountains, Vancouver Canada. Geomorphology 393:107921. https://doi.org/10.1016/J.GEOMORPH.2021.107921

Jones JN, Boulton SJ, Stokes M, Bennett GL, Whitworth MRZ (2021) 30-year record of Himalaya mass-wasting reveals landscape perturbations by extreme events. Nat Commun 12(1):1–15. https://doi.org/10.1038/s41467-021-26964-8

Kansakar SR, Hannah DM, Gerrard J, Rees G (2004) Spatial pattern in the precipitation regime of Nepal. Int J Climatol 24(13):1645–1659. https://doi.org/10.1002/JOC.1098

Karmacharya M (1989) Landslide in Nepal in the period 1970–1980. Tribhuvan University, Kathmandu

Kc R, Aryal M, Dahal BK, Sharma K (2021) Spatial and temporal analysis of landslides during last decade in Nepal. In: Proceedings of 10th IOE Graduate Conference, pp 102–106. https://www.researchgate.net/publication/358987469_Spatial_and_Temporal_Analysis_of_Landslides_during_Last_Decade_in_Nepal

Kendall MG (1948) The advanced theory of statistics, 4th edn. Springer, Cham

Kirschbaum D, Stanley T, Zhou Y (2015) Spatial and temporal analysis of a global landslide catalog. Geomorphology 249:4–15. https://doi.org/10.1016/j.geomorph.2015.03.016

Lin Q, Wang Y (2018) Spatial and temporal analysis of a fatal landslide inventory in China from 1950 to 2016. Landslides 15(12):2357–2372. https://doi.org/10.1007/s10346-018-1037-6

Lin CW, Liu SH, Lee SY, Liu CC (2006) Impacts of the Chi-Chi earthquake on subsequent rainfall-induced landslides in central Taiwan. Eng Geol 86(2–3):87–101. https://doi.org/10.1016/J.ENGGEO.2006.02.010

Malamud BD, Turcotte DL, Guzzetti F, Reichenbach P (2004) Landslide inventories and their statistical properties. Earth Surf Proc Land 29(6):687–711. https://doi.org/10.1002/esp.1064

Mann HB (1945) Nonparametric tests against trend. Econometrica 13(3):245. https://doi.org/10.2307/1907187

Marc O, Hovius N, Meunier P, Gorum T, Uchida T (2016) A seismologically consistent expression for the total area and volume of earthquake-triggered landsliding. J Geophys Res Earth Surf 121(4):640–663. https://doi.org/10.1002/2015JF003732

McAdoo BG, Quak M, Gnyawali KR, Adhikari BR, Devkota S, Lal Rajbhandari P, Sudmeier-Rieux K (2018) Roads and landslides in Nepal: how development affects environmental risk. Nat Hazard 18(12):3203–3210. https://doi.org/10.5194/nhess-18-3203-2018

Ministry of Irrigation (2014) Report on Jure landslide, Mankha VDC, Sindhupalchowk District

Nadim F, Kjekstad O, Peduzzi P, Herold C, Jaedicke C (2006) Global landslide and avalanche hotspots. Landslides 3(2):159–173. https://doi.org/10.1007/s10346-006-0036-1

Nepal Disaster Risk Reduction Portal (2023). http://drrportal.gov.np/. Retrieved 18 May 2021

Parker RN, Hancox GT, Petley DN, Massey CI, Densmore AL, Rosser NJ (2015) Spatial distributions of earthquake-induced landslides and hillslope preconditioning in the northwest South Island New Zealand. Earth Surf Dyn 3(4):501–525. https://doi.org/10.5194/ESURF-3-501-2015

Paudel KP, Andersen P (2013) Response of rangeland vegetation to snow cover dynamics in Nepal Trans Himalaya. Clim Change 117(1–2):149–162. https://doi.org/10.1007/S10584-012-0562-X/METRICS

Pennington C, Freeborough K, Dashwood C, Dijkstra T, Lawrie K (2015) The National Landslide Database of Great Britain: Acquisition, communication and the role of social media. Geomorphology 249:44–51. https://doi.org/10.1016/j.geomorph.2015.03.013

Pereira S, Zêzere JL, Quaresma I, Santos PP, Santos M (2016) Mortality Patterns of Hydro-Geomorphologic Disasters. Risk Anal 36(6):1188–1210. https://doi.org/10.1111/risa.12516

Petley D (2012) Global patterns of loss of life from landslides. Geology 40(10):927–930. https://doi.org/10.1130/G33217.1

Petley DN, Hearn GJ, Hart A, Rosser NJ, Dunning SA, Oven K, Mitchell WA (2007) Trends in landslide occurrence in Nepal. Nat Hazards 43(1):23–44. https://doi.org/10.1007/s11069-006-9100-3

Pirasteh S, Li J (2016) Landslides investigations from geoinformatics perspective: quality, challenges, and recommendations. Geomat Nat Haz Risk 8(2):448–465. https://doi.org/10.1080/19475705.2016.1238850

Pradhan B, Singh RP, Buchroithner MF (2006) Estimation of stress and its use in evaluation of landslide prone regions using remote sensing data. Adv Space Res 37(4):698–709. https://doi.org/10.1016/J.ASR.2005.03.137

Qiu H, Cui Y, Hu S, Yang D, Pei Y, Yang W (2019a) Temporal and spatial distributions of landslides in the Qinba Mountains, Shaanxi Province, China. Geomat Nat Haz Risk 10(1):599–621. https://doi.org/10.1080/19475705.2018.1536080

Qiu H, Cui Y, Yang D, Pei Y, Hu S, Ma S, Hao J, Liu Z (2019b) Spatiotemporal Distribution of Nonseismic Landslides during the Last 22 Years in Shaanxi Province China. ISPRS Int J Geo-Inf 8(11):505. https://doi.org/10.3390/ijgi8110505

Qiu H, Hu S, Yang D, He Y, Pei Y, Kamp U (2020) Comparing landslide size probability distribution at the landscape scale (Loess Plateau and the Qinba Mountains, Central China) using double Pareto and inverse gamma. Bull Eng Geol Env 80(2):1035–1046. https://doi.org/10.1007/s10064-020-02037-w

Roberts S, Jones JN, Boulton SJ (2021) Characteristics of landslide path dependency revealed through multiple resolution landslide inventories in the Nepal Himalaya. Geomorphology 390:107868. https://doi.org/10.1016/J.GEOMORPH.2021.107868

Rossi M, Witt A, Guzzetti F, Malamud BD, Peruccacci S (2010) Analysis of historical landslide time series in the Emilia-Romagna region, northern Italy. Earth Surf Proc Land 35(10):1123–1137. https://doi.org/10.1002/ESP.1858

Samia J, Temme A, Bregt A, Wallinga J, Guzzetti F, Ardizzone F, Rossi M (2017) Do landslides follow landslides? Insights in path dependency from a multi-temporal landslide inventory. Landslides 14(2):547–558. https://doi.org/10.1007/S10346-016-0739-X/FIGURES/10

Scott LM, Janikas MV (2010) Spatial statistics in ArcGIS. Handbook of applied spatial analysis. Springer, Berlin, pp 27–41

Sen PK (1968) Estimates of the regression coefficient based on Kendall's Tau. J Am Stat Assoc 63(324):1379–1389. https://doi.org/10.1080/01621459.1968.10480934

Sepúlveda SA, Petley DN (2015) Regional trends and controlling factors of fatal landslides in Latin America and the Caribbean. Nat Hazard 15(8):1821–1833. https://doi.org/10.5194/nhess-15-1821-2015

Shafique M (2020) Spatial and temporal evolution of co-seismic landslides after the 2005 Kashmir earthquake. Geomorphology 362:107228. https://doi.org/10.1016/J.GEOMORPH.2020.107228

Shahid S (2011) Trends in extreme rainfall events of Bangladesh. Theoret Appl Climatol 104(3–4):489–499. https://doi.org/10.1007/s00704-010-0363-y

Sharma K, Subedi M, Acharya I, Pokharel B (2018) Geotechnical and structural aspect of 2015 Gorkha Nepal earthquake and lesson learnt. J Inst Eng. https://doi.org/10.3126/jie.v13i1.20345

Silverman BW (2018) Density estimation: For statistics and data analysis. CRC Press. https://doi.org/10.1201/9781315140919

Tang C, Van Westen CJ, Tanyas H, Jetten VG (2016) Analysing post-earthquake landslide activity using multi-temporal landslide inventories near the epicentral area of the 2008 Wenchuan earthquake. Nat Hazard 16(12):2641–2655. https://doi.org/10.5194/NHESS-16-2641-2016

Temme A, Guzzetti F, Samia J, Mirus BB (2020) The future of landslides' past—a framework for assessing consecutive landsliding systems. Landslides 17(7):1519–1528. https://doi.org/10.1007/S10346-020-01405-7/METRICS

Timilsina M, Bhandary NP, Dahal RK, Yatabe R (2014) Distribution probability of large-scale landslides in central Nepal. Geomorphology 226:236–248. https://doi.org/10.1016/J.GEOMORPH.2014.05.031

Tiwari B, Ajmera B, Dhital S, Sitoula NR (2017) Landslides Induced by the 2015 Gorkha Earthquake. Adv Cult Liv Landslides. https://doi.org/10.1007/978-3-319-53498-5_94

Tonini M, Abellan A (2014) Rockfall detection from terrestrial lidar point clouds: a clustering approach using R. J Spat Inf Sci 8(1):95–110. https://doi.org/10.5311/JOSIS.2014.8.123

Tonini M, Pecoraro G, Romailler K, Calvello M (2020) Spatio-temporal cluster analysis of recent italian landslides. Georisk. https://doi.org/10.1080/17499518.2020.1861634

Vakhshoori V, Zare M (2016) Landslide susceptibility mapping by comparing weight of evidence, fuzzy logic, and frequency ratio methods. Geomat Nat Haz Risk 7(5):1731–1752. https://doi.org/10.1080/19475705.2016.1144655

Valagussa A, Frattini P, Valbuzzi E, Crosta GB (2021) Role of landslides on the volume balance of the Nepal 2015 earthquake sequence. Sci Rep 11(1):1–12. https://doi.org/10.1038/s41598-021-83037-y

Witt A, Malamud BD, Rossi M, Guzzetti F, Peruccacci S (2010) Temporal correlations and clustering of landslides. Earth Surf Proc Land 35(10):1138–1156. https://doi.org/10.1002/ESP.1998

World Bank Open Data (2023) https://data.worldbank.org/

Xie Z, Yan J (2008) Kernel Density Estimation of traffic accidents in a network space. Comput Environ Urban Syst 32(5):396–406. https://doi.org/10.1016/j.compenvurbsys.2008.05.001

Zhang F, Huang X (2018) Trend and spatiotemporal distribution of fatal landslides triggered by non-seismic effects in China. Landslides 15(8):1663–1674. https://doi.org/10.1007/s10346-018-1007-z

Zhang SL, Lv PF, Yang XG, Chen XZ, Zhou JW (2018) Spatiotemporal distribution and failure mechanism analyses of reservoir landslides in the Dagangshan reservoir, south-west China. Geomat Nat Haz Risk 9(1):791–815. https://doi.org/10.1080/19475705.2018.1480536

Zhu D, Song K, Mu J, Huang H, Du H, Xiazhuang F, Sun C (2021) Effect of climate change induced extreme precipitation on landslide activity in the Three Gorges Reservoir, China. Bull Eng Geol Env 80(2):781–794. https://doi.org/10.1007/S10064-020-01948-Y

Zuo R, Agterberg FP, Cheng Q, Yao L (2009) Fractal characterization of the spatial distribution of geological point processes. Int J Appl Earth Obs Geoinf 11(6):394–402. https://doi.org/10.1016/j.jag.2009.07.001